MARIN

Maritime Research Institute Netherlands

18

2 Haagsteeg P.O. Box 28
6700 AA Wageningen The Netherlands
Telephone +31 8370 49911 Telex 45148 mmb nl
Telefax +31 8370 [illegible]

C60797 - WORKSHOP OE

THE PREDICTION OF THE BEHAVIOUR OF SINGLE POINT MOORED TANKERS

By: J.E.W. Wichers (MARIN)

September 1987.

E PREDICTION OF THE BEHAVIOUR OF SINGLE POINT MOORED TANKERS

E.W. Wichers

ritime Research Institute Netherlands (MARIN)

SUMMARY

A tanker moored by means of a bow hawser to a fixed pile will be considered. To determine the low frequency part of the mooring forces the low frequency motions of the tanker have to be known. In the equations of motion the low frequency hydrodynamic damping forces are dominated by viscosity. No mathematical model exists to determine completely these values. Therefore model experiments were carried out in calm water and in current to determine the magnitude of these damping forces. To evaluate the derived low frequency viscous damping terms in the equations of motion time domain simulations were performed. For the no-current condition the tanker was exposed to regular waves. Large unstable motions in the horizontal plane were obtained. For large amplitude motions in a current field unstable conditions can be found by using the Routh criterion. For current and wind unstable conditions were found, for which time domain simulations with large amplitudes of the tanker motions were performed. The computed results are compared with the results of model tests.

INTRODUCTION

A single point moored tanker exposed to :regular waves, wind and current will un-:rgo not only low frequency surge motions, it in general will perform low frequency ›tions in the horizontal plane. The equa-:ons of motion will be governed by the low :equency force components as is shown in :g. 1.

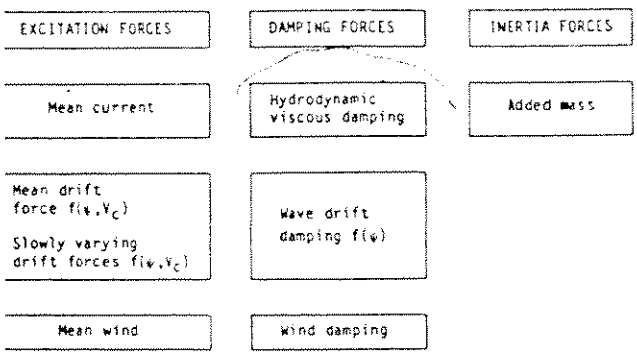

ig.1. The low frequency force components

Information on the current speed dependent wave drift force and the wave drift damping force can be found in ref. [1], [2] and [3].

In the establisment of the equations of motion difficulties arise in the description of the low frequency reaction forces and moment. In the considered low frequency range the damping parts of the hydrodynamic reaction forces and moments cannot be attributed to forces of potential nature only, but are for an important part determined by viscosity. The forces and moments caused by viscosity cannot be fully solved by mathematical models but have to be determined by means of model tests. For the determination of the low frequency damping forces the following set of model tests have been carried out:

surge mode	sway mode	yaw mode
oscillatory motions in calm water		
steady linear motions/steady current forces		
oscillatory motions in current		

A clear distinction will be made between e damping forces and moment in calm water d in current. By means of the results of he experiments a description of the damping orces and moment in calm (still) water and current can be derived.

In formulating the equations of the low requency motions many investigations have een carried out. No formulation was found r the case of calm water. The formulations case of current has been compared with lescriptions given by others, for instance f. [4], [5] and [6] and reported in ref.]. To evaluate the present formulation on he low frequency damping forces and moment he equations of motion have been solved in e time domain. For the purpose of evaluaon some specific weather conditions have been applied. The computed results are compared with the results of model tests.

EQUATIONS OF MOTION OF THE LOW FREQUENCY MOTIONS

To study the motions of the vessel in the degrees of freedom (in the horizontal plane) use has been made of two different systems of co-ordinates as is indicated in g. 2:

the system of axis Ox(1)x(2) is fixed to earth;

the frame Gx_1x_2 is linked to the vessel in which the origin corresponds with the centre of gravity of the vessel.

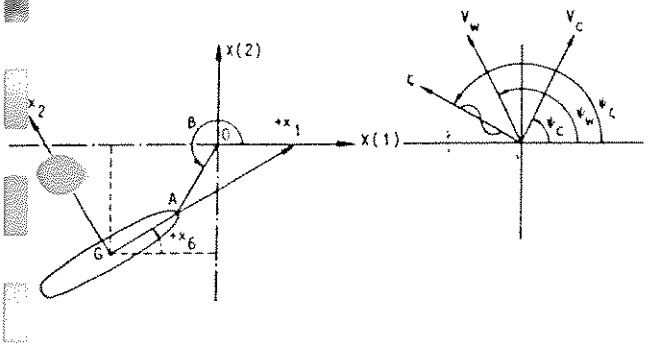

Fig. 2. System of co-ordinates of a tanker moored to an SPM and sign convention of weather directions

Based on the earth fixed system of co-dinates the differential equations of motion according to Newton's second law are:

$$MX(1) = X(1)$$

$$MX(2) = X(2) \qquad (1)$$

$$IX(6) = X(6)$$

in which:
M = mass of the tanker
I = moment of inertia of the tanker.

In literature the ship's manoeuvrability is mostly described by a set of differential equations of motion relative to a ship-fixed system of co-ordinates. The transformation to the ship-fixed system of co-ordinates has the following consequences:

$$\underline{X}(j) = T\,\underline{X}_j \qquad \text{for } j = 1,2,6 \qquad (2)$$

$$\dot{\underline{x}}(j) = T\,\dot{\underline{x}}_j \qquad (3)$$

where:

$$T = \begin{vmatrix} \cos x_6 & -\sin x_6 & 0 \\ \sin x_6 & \cos x_6 & 0 \\ 0 & 0 & 1 \end{vmatrix}$$

while for the acceleration the following transformation will be found:

$$\ddot{\underline{x}}(j) = T\,\ddot{\underline{x}}_j + \dot{T}\,\dot{\underline{x}}_j \qquad (4)$$

Substituting (2) and (4) in (1) yield the equations of motion for the ship-fixed system of co-ordinates:

$$\begin{aligned} M(\ddot{x}_1 - \dot{x}_2\dot{x}_6) &= X_1 \\ M(\ddot{x}_2 + \dot{x}_1\dot{x}_6) &= X_2 \\ I\ddot{x}_6 &= X_6 \end{aligned} \qquad (5)$$

For the low frequency motion components x_1, x_2 and x_6 the complete equations of motion for the ship bound system of axes are:

$$M(\ddot{\underline{x}}+D\dot{\underline{x}}) = \underline{X}_H + \underline{X}_W + \underline{X}_M + \underline{X}_D + \underline{X}_T \qquad (6)$$

where:

$$\underline{x} = \begin{Bmatrix} x_1 \\ x_2 \\ x_6 \end{Bmatrix}$$

$$M = \begin{vmatrix} M & 0 & 0 \\ 0 & M & 0 \\ 0 & 0 & I_6 \end{vmatrix}$$

$$D = \begin{vmatrix} 0 & 0 & -\dot{x}_2 \\ 0 & 0 & +\dot{x}_1 \\ 0 & 0 & 0 \end{vmatrix}$$

$\underline{X}_H$ = hydrodynamic reaction and current forces
$\underline{X}_W$ = wind forces
$\underline{X}_M$ = mooring forces
$\underline{X}_D$ = wave drift forces
$\underline{X}_T$ = thrust of main and auxiliary propellers.

The hydrodynamic forces $\underline{X}_H$ arise from changes in the relative motions of the ship and the surrounding fluid. In unrestricted water the forces are independent of the coordinates x(1) and x(2). Further according to classical hydrodynamic theory the hydrodynamic forces will not be dependent on higher derivatives of the displacement than the second:

$$\underline{X}_H = f(u,v,x_6(u,v),x_6,\dot{\underline{x}},\ddot{\underline{x}}) \qquad (7)$$

in which:
u,v = steady state drift velocity
$x_6(u,v)$ = steady state drift angle.

Expansion in a Taylor series about the steady state condition the hydrodynamic forces and moment are:

$$\underline{X}_H = \sum_{n=0}^{\infty} \frac{1}{n!}\Big[x_6\frac{\partial}{\partial x_6} + \dot{x}_1\frac{\partial}{\partial \dot{x}_1} + \dot{x}_2\frac{\partial}{\partial \dot{x}_2} + \dot{x}_6\frac{\partial}{\partial \dot{x}_6} + \ddot{x}_1\frac{\partial}{\partial \ddot{x}_1} + \ddot{x}_2\frac{\partial}{\partial \ddot{x}_2} + \ddot{x}_6\frac{\partial}{\partial \ddot{x}_6}\Big]^n * f(u,v,x_6(u,v),x_6,\dot{\underline{x}},\ddot{\underline{x}})\Big|_{x_6=0,\dot{\underline{x}}=0,\ddot{\underline{x}}=0} \qquad (8)$$

If the expansion is carried out for the first and higher order terms it results in a number of terms, the coefficients of which, in general, are assumed to be constant while the magnitudes have to be determined by means of model tests or calculations.

Contrary to normal manoeuvring application (high speed, high rate of turning) for a tanker moored to an SPM system specific requirements have to be fulfilled, viz.:
- large drift angles (0-360 degrees)
- small values of the drift velocities (current speed)
- small values of oscillating rates of turning
- for zero rate of turning the hydrodynamic forces have to correspond to the steady current forces.

To obtain the SPM manoeuvring coefficients specific model experiments were carried out to determine the viscous resistance terms while the hydrodynamic inertia terms were computed by means of 3-D potential theory, see ref. [8].

3. TANKER

For the experiments and the computations a 200 kTDW tanker was considered. The particulars of the vessel for different loading conditions are given in Table 1. Besides the particulars also the coefficients of the added mass for the frequencies approaching zero are given. The body plan of the tanker is shown in Fig. 3.

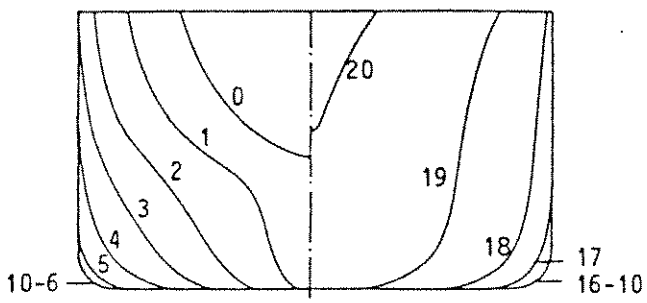

Fig. 3. Body plan of the tanker

4. EQUATIONS OF MOTION IN CALM WATER

In deriving the low frequency fluid reactive forces in calm water, the external force $\underline{X}_H$ in eq. (6) will be considered only:

$$M(\ddot{\underline{x}}+D\dot{\underline{x}}) = \underline{X}_H \qquad (9)$$

Because of the low frequency motions it can be assumed that the disturbances of the free fluid surface are negligible. Assuming an irrotational and ideal fluid, Norrbin [9] derived for the forces exerted on the vessel:

$$\begin{aligned} X_{1H} &= -a_{11}\ddot{x}_1 + a_{22}\dot{x}_2\dot{x}_6 + a_{26}\dot{x}_6^2 \\ X_{2H} &= -a_{22}\ddot{x}_2 - a_{11}\dot{x}_1\dot{x}_6 - a_{26}\ddot{x}_6 \\ X_{6H} &= -a_{66}\ddot{x}_6 - (a_{22}-a_{11})\dot{x}_1\dot{x}_2 + \\ &\quad - a_{62}(\ddot{x}_2+\dot{x}_1\dot{x}_6) \end{aligned} \qquad (10)$$

where a_{kj} = added mass coefficient at low frequency.

The mentioned equations lead to the well-known d'Alembert paradox because the right-hand sides are equal to zero for:

$$\ddot{x}_1 = \ddot{x}_2 = \dot{x}_6 = 0$$

The term $-(a_{22}-a_{11})\dot{x}_1\dot{x}_2$ is the only arising in an ideal fluid and often referred to as the Munk-moment.

In a real fluid, however, viscosity is involved. The viscosity leads to modifications of the velocity dependent terms and/or introduces additional damping terms. Further it may be assumed that the acceleration dependent terms are hardly affected by viscosity. For the equations of motion the following formulations are assumed:

Table 1
The particulars of the tanker

Designation	Symbol	Unit	Magnitude		
			Loaded	Inter-mediate	Ballasted
ding condition			100%	60%	25%
raft in per cent of ded draft			100%	70%	40%
gth between perpendiculars	L_{pp}	m	310.00	310.00	310.00
eadth	B	m	47.17	47.17	47.17
epth	H	m	29.70	29.70	29.70
ft	T	m	18.90	13.23	7.56
ted area	S	m^2	22,804	18,670	13,902
isplacement volume	∇	m^3	234,994	159,698	88,956
lass	M	tfs^2/m	24,553	16,686	9,295
tre of buoyancy forward tion 10	$\overline{FB}$	m	6.6	9.04	10.46
entre of gravity above keel	$\overline{KG}$	m	13.32	11.55	13.32
letacentric height transverse	$\overline{GM}_t$	m	5.78	8.66	13.94
tacentric height ngitudinal	$\overline{GM}_l$	m	403.83	-	-
Transverse radius of ration in air	k_{11}	m	14.77	15.02	15.30
ngitudinal radius of ration in air	k_{22}	m	77.47	77.52	82.15
law radius of gyration in air	k_{66}	m	79.30	83.81	83.90
nd area of superstructure (aft):					
- lateral area	A_{LS}	m^2	922	922	922
- transverse area	A_{TS}	m^2	853	853	853
ded mass	a_{11}	tfs^2/m	1,594	755	250
= 0 rad/s	a_{22}	tfs^2/m	25,092	10,940	5,375
(water depth 82.5 m)	a_{26}	tfs^2	-83,618	-30,400	-16,132
	a_{62}	tfs^2	-83,618	-30,400	-16,132
	a_{66}	$tfms^2$	123,510,000	59,607,700	23,200,000

$$
\begin{aligned}
&(M+a_{11})\ddot{x}_1 = \\
&= (M+a_{22})\dot{x}_2\dot{x}_6 + a_{26}\dot{x}_6^2 + X_{1SW} \\
&(M+a_{22})\ddot{x}_2 + a_{26}\ddot{x}_6 = \\
&= -(M+a_{11})\dot{x}_1\dot{x}_6 + X_{2SW} \qquad (11) \\
&(I+a_{66})\ddot{x}_6 + a_{62}\ddot{x}_2 = \\
&= -(a_{22}-a_{11})\dot{x}_1\dot{x}_2 - a_{62}\dot{x}_1\dot{x}_6 + X_{6SW}
\end{aligned}
$$

which X_{1SW}, X_{2SW} and X_{6SW} are the low equency viscous fluid resistance force/ oment components in calm water. The low requency viscous fluid resistance terms ill be determined by means of experiments.

4.1 Viscous damping in calm water due to surge motion

Computations by means of 3-D potential diffraction theory have shown that the radiated damping can be neglected for $2\pi/T\sqrt{L/g} < 0.5$, see ref. [10]. This means that for low frequencies the frictional mechanism in the boundary layer dominates the damping.

Since in the low frequency range the oscillating amplitudes will be large, the relative current force concept is normally used. By applying this concept, however, it is assumed that the boundary layer is turbulent. Physical extinction tests with the loaded 200 kTDW in 82.5 m water depth (scale 1:82.5) show that the relative current force concept is not allowed in calm water, see

ref. [7]. By applying the linearized equations of Navier-Stokes no satisfactory results were obtained. In order to obtain the damping coefficients for the surge mode of motion experiments have been carried out. Extinction tests for various vessel types and spring constants were performed. The results, scaled according to Froude's law of similitude are presented in Fig. 4.

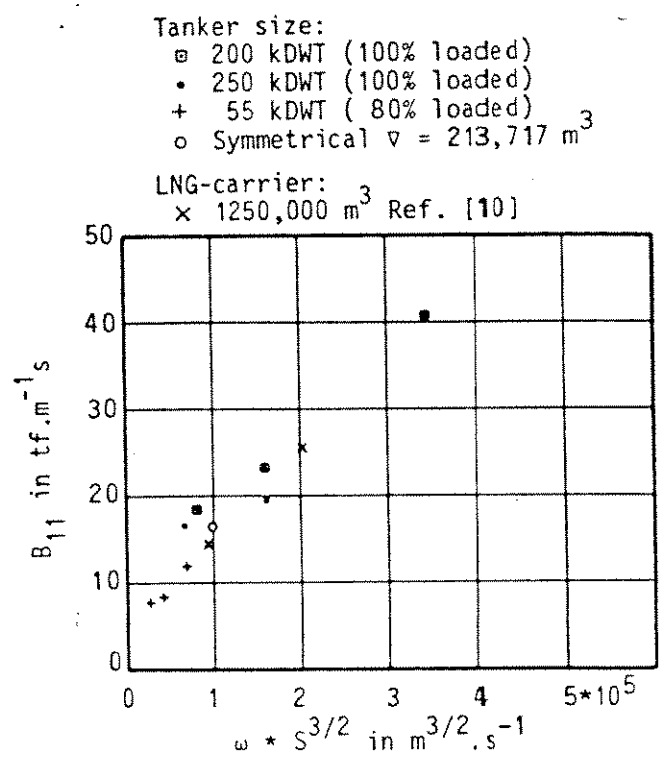

Fig. 4. Measured viscous damping coefficients for the surge mode of motion as function of wetted hull area and surge frequency

4.2 Viscous damping in calm water due to sway and yaw mode of motion

In order to determine the viscous resistance force/moment components caused by the sway and yaw modes of motion, Planar Motion Mechanism tests as is described in ref. [7] have been carried out. Instead of employing the coefficients as can be derived from the Taylor expansion, see eq. (8), the procedure is followed as is indicated in ref. [7]. Following this concept the distribution of the viscous resistance coefficient over the length of the vessel can be estimated. The results for both the loaded and the ballasted 200 kTDW tanker in 82.5 m of water depth are presented in Fig. 5.

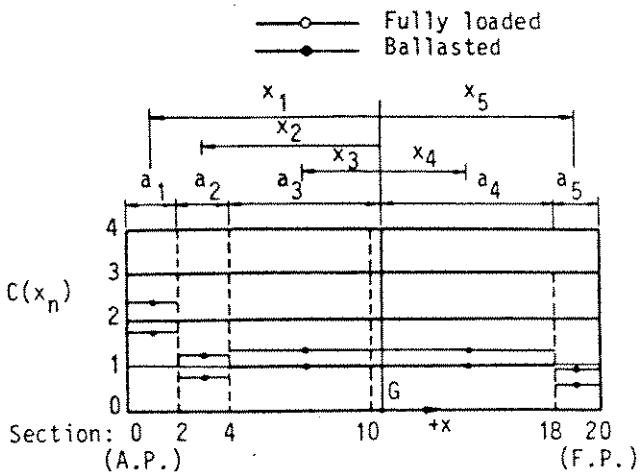

Fig. 5. Transverse resistance coefficient as function of the longitudinal position along the tanker centre line

Applying the assumed distribution of the transverse viscous fluid resistance coefficients over the length of the vessel, the low frequency resistance forces/moment assuming a decoupling in surge direction can be described as follows:

$$X_{1SW} = -B_{11}\,\dot{x}_1$$

$$X_{2SW} = -\tfrac{1}{2}\rho_w T \sum_{n=1}^{5} C(x_n)(\dot{x}_2+\dot{x}_6 x_n)\,|\dot{x}_2+\dot{x}_6 x_n|\,a_n$$

$$X_{6SW} = -\tfrac{1}{2}\rho_w T \sum_{n=1}^{5} C(x_n)(\dot{x}_2+\dot{x}_6 x_n)\,|\dot{x}_2+\dot{x}_6 x_n|\,x_n a_n \qquad (12)$$

It must be emphasized that using the resistance coefficient obtained from steady current force measurements at a current angle of 90 degrees as may be applied in the past for an oscillating motion in calm water leads to an underestimate of the resistance force.

5. BOW HAWSER MOORED TANKER EXPOSED TO REGULAR WAVES

To evaluate the viscous damping values in calm water the low frequency motions of a tanker (3 D.O.F.) moored by means of a bow hawser and exposed to regular long-crested waves have been computed. The results have been compared with the results of model tests. The tanker concerns the loaded 200 kTDW tanker moored in 82.5 m water depth.

The bow hawser was connected to a fixed ile. The length of the unloaded hawser amounts to 75 m. The non-linear load deflection curve is shown in Fig. 6.

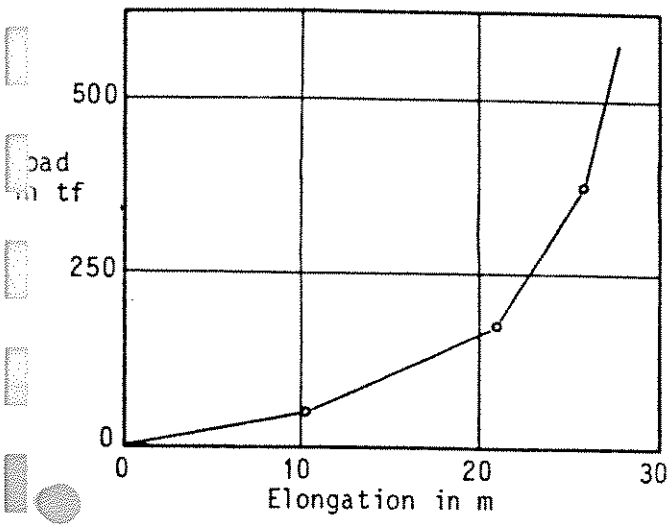

ig. 6. Bow hawser load-elongation characteristic

or the regular waves the following characteristics were used:

T in s	$2\zeta_a$ in m
6.45	4.74 - 2.75
7.14	4.72 - 3.23
8.00*	5.00 - 3.00
9.10	4.98 - 3.07

* theory only

5.1 Computations

Referring to eq. (6) and eq. (11) the complete equations of motion can be written as follows:

$$
\begin{aligned}
&M(\ddot{x}_1 - \dot{x}_2\dot{x}_6) = \\
&= X_{1P} + X_{1SW} + \bar{X}_1(\psi_{\zeta r}) - \bar{B}_1\dot{x}_1 + X_{1M} \\
&m(\ddot{x}_2 + \dot{x}_1\dot{x}_6) = \\
&= X_{2P} + X_{2SW} + \bar{X}_2(\psi_{\zeta r}) - \bar{B}_2\dot{x}_2 + X_{2M} \\
&I\ddot{x}_6 = \\
&= X_{6P} + X_{6SW} + \bar{X}_6(\psi_{\zeta r}) - \bar{B}_6\dot{x}_6 + X_{6M}
\end{aligned}
\qquad (13)
$$

in which:

X_{np} = potential inertia parts of the reaction forces/moment

X_{nSW} = viscous parts of the reaction forces/moment

$X_n(\psi_{\zeta r})$ = mean wave drift forces/moment in a regular wave as function of $\psi_{\zeta r}$

$\psi_{\zeta r}$ = $\psi_\zeta - x_6$ = relative wave angle

$\bar{B}_n$ = mean wave drift damping coefficient in a regular wave

X_{nm} = mooring force components caused by the bow hawser

n = 1,2,6.

The wave direction ψ_ζ as defined in Fig. 2 was 180 degrees.

The potential inertia parts of the reaction forces/moment are given in eq. (11), while the values of the coefficients are presented in Table 1. The coefficients of the viscous part in surge direction can be found in Fig. 4, while the values of the transverse resistance coefficients can be read from Fig. 5.

The mean wave drift forces/moment in the regular waves as function of the relative wave angle have been derived from the data given in Fig. 7. The quadratic transfer functions have been computed by means of the direct pressure integration method, see ref. [11]. For the mean wave drift damping coefficient in the regular waves a constant coefficient $\bar{B}_1$ is taken into account only. The value is derived from the quadratic transfer function as is given in ref. [7]. With regard to the value of the calm water damping B_{11} the value of $\bar{B}_1$ contributes significantly. It is assumed that for the sway and yaw mode of motions the mean wave drift damping is small with regard to the appropriate viscous damping, see ref. [3], and is therefore deleted.

5.2 Model tests

During the model tests the horizontal motions at point A (= fairlead) were measured in an earth-fixed system of co-ordinates as indicated in Fig. 2. Furthermore the yaw motion and the hawser force were recorded. Both the linear and the rotational motions were measured by means of optical tracking devices.

The SPM model tests were carried out in the Wave and Current Laboratory of MARIN measuring 60 by 40 m at a water depth of 1 m. The model scale was 1:82.5.

5.3 Results of computations and model tests

The initial conditions for both the computations and the model tests were the same. Under influence of the environment the tanker was kept under the following start condition:

x_6 = 7.5 degrees

$x_A(2)$ = 0 m

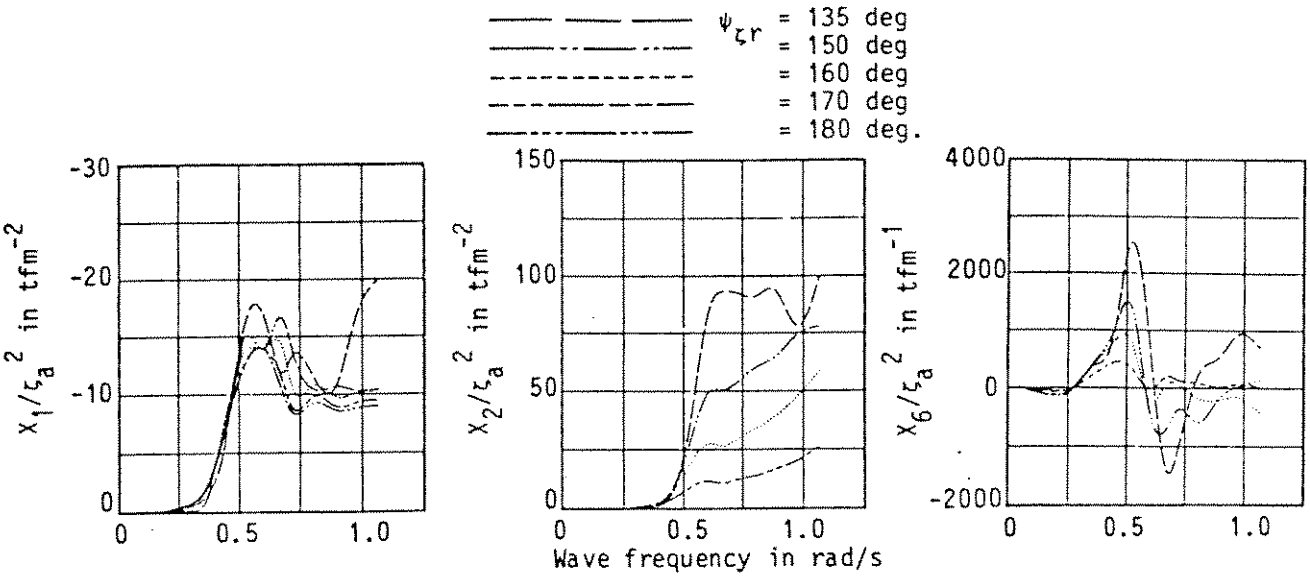

Fig. 7. The quadratic transfer function of the wave drift force in x_1, x_2 and x_6 direction as function of relative wave direction

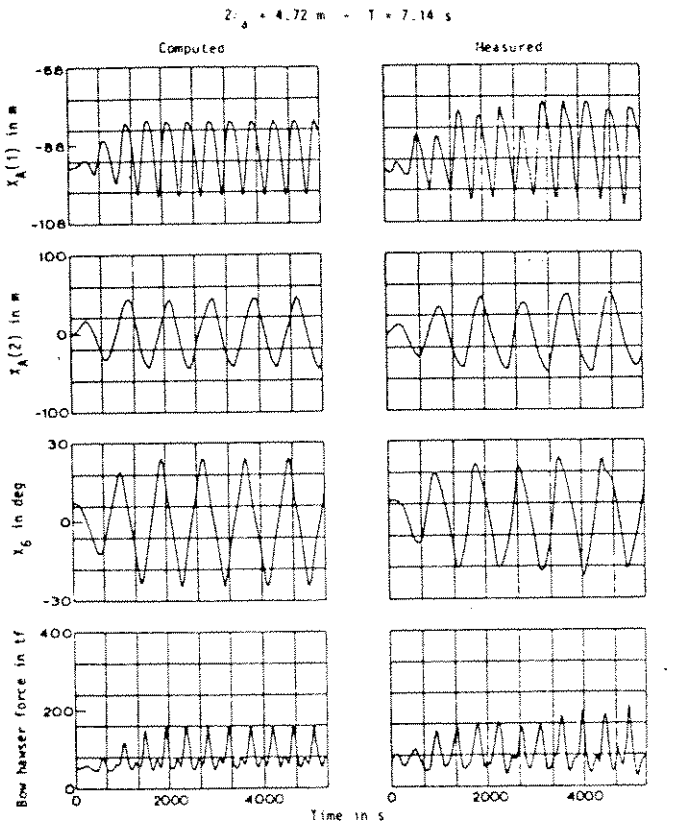

Fig. 8. Time domain results from simulation and model tests

and in the $x_A(1)$-direction restrained by the bow hawser force, see Fig. 2. At t=0 the tanker was released. In Fig. 8 the comparison of the results of the simulation and the model test is presented for $2\zeta_a$ = 4.72 m and T = 7.14 s. As a result of the unstable behaviour of the system the dynamic loads in the hawser increase to 160 tf instead of 49 tf as results from the static calculation. Of the steady parts of the computations and measurements some results are plotted in Fig. 9. A good agreement was found between the computed and measured results.

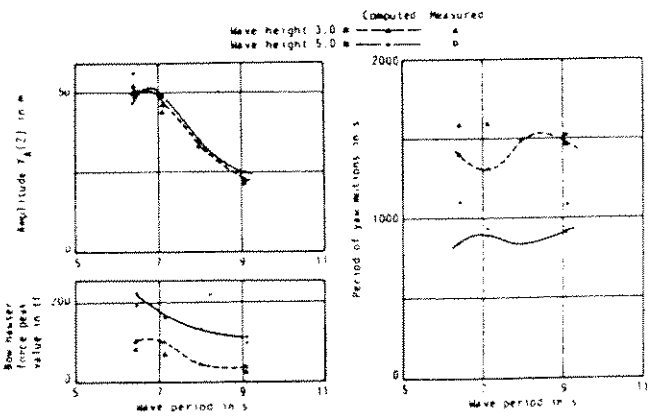

Fig. 9. Results of computations and model tests

6. EQUATIONS OF MOTION IN CURRENT

In deriving the low frequency fluid reactive forces in current, the external force $\underline{X}_H$ in eq. (6) will be considered only:

$$M(\ddot{\underline{x}}+D\dot{\underline{x}}) = \underline{X}_H \tag{14}$$

The relative velocity of the vessel with respect to the fluid is:

$$V_{cr} = (u_r^2+v_r^2)^{\frac{1}{2}} \tag{15}$$

in which the relative velocity components will be:

$$\begin{aligned} u_r &= \dot{x}_1 - V_c \cos(\psi_c - x_6) \\ v_r &= \dot{x}_2 - V_c \sin(\psi_c - x_6) \end{aligned} \tag{16}$$

and the relative acceleration components:

$$\begin{aligned} \dot{u}_r &= \ddot{x}_1 - V_c \dot{x}_6 \sin(\psi_c - x_6) \\ \dot{v}_r &= \ddot{x}_2 + V_c \dot{x}_6 \cos(\psi_c - x_6) \end{aligned} \tag{17}$$

while:
V_c = current velocity
ψ_c = current direction
x_6 = yaw angle in global co-ordinates.

Because of the low frequency motions it can be assumed that the disturbances of the free fluid surface are negligible. Assuming an ideal fluid, Norrbin [9] derived for the forces exerted on the vessel:

$$\begin{aligned} X_{1H} &= - a_{11}\dot{u}_r + a_{22}v_r\dot{x}_6 + a_{26}\dot{x}_6^2 \\ X_{2H} &= - a_{22}\dot{v}_r - a_{11}u_r\dot{x}_6 - a_{26}\ddot{x}_6 \\ X_{6H} &= - a_{66}\ddot{x}_6 - (a_{22}-a_{11})u_rv_r + \\ &\quad - a_{62}(\dot{v}_r+u_r\dot{x}_6) \end{aligned} \tag{18}$$

where a_{kj} = added mass coefficient at low frequency, or following equations (16), (17) and (18):

$$\begin{aligned} X_{1H} &= - a_{11}\ddot{x}_1 - (a_{22}-a_{11})V_c * \\ &\quad * \sin(\psi_c-x_6)\dot{x}_6 + a_{22}\dot{x}_2\dot{x}_6 + a_{26}\dot{x}_6^2 \\ X_{2H} &= - a_{22}\ddot{x}_2 - a_{26}\ddot{x}_6 - (a_{22}-a_{11})V_c * \\ &\quad * \cos(\psi_c-x_6)\dot{x}_6 - a_{11}\dot{x}_1\dot{x}_6 \\ X_{6H} &= - a_{66}\ddot{x}_6 - a_{62}\ddot{x}_2 - (a_{22}-a_{11})u_rv_r + \\ &\quad - a_{62}\dot{x}_1\dot{x}_6 \end{aligned} \tag{19}$$

The mentioned equations lead to the well-known d'Alembert paradox because the right-hand sides are equal to zero for $\ddot{x}_1 = \ddot{x}_2 = \dot{x}_6 = 0$. The term $-(a_{22}-a_{11})u_rv_r$ is only arising in an ideal fluid and often referred to as the Munk-moment.

In a real fluid, however, viscosity is involved. The viscosity leads to modifications of the velocity dependent terms and/or introduces additional damping (resistance) terms. Further it may be assumed that the acceleration dependent terms are hardly affected by viscosity.

Replacing the destabilizing Munk-moment by the steady current moment formulation and neglecting the small contributions of $a_{26}\dot{x}_6^2$ and $a_{62}\dot{x}_1\dot{x}_6$ in respectively the x_1 direction and x_6 direction we rewrite the equation by the following formulation combining expressions for a real and ideal fluid:

$$\begin{aligned} (M+a_{11})\ddot{x}_1 &= (M+a_{22})\dot{x}_2\dot{x}_6 + \\ &\quad + X_{1stat} + X_{1dyn} \\ (M+a_{22})\ddot{x}_2 + a_{26}\ddot{x}_6 &= - (M+a_{11})\dot{x}_1\dot{x}_6 + \\ &\quad + X_{2stat} + X_{2dyn} \\ (I_6+a_{66})\ddot{x}_6 + a_{62}\ddot{x}_2 &= X_{6stat} + X_{6dyn} \end{aligned} \tag{20}$$

in which:

$$\begin{aligned} X_{1stat} &= \tfrac{1}{2}\rho_w L T C_1(\psi_{cr})V_{cr}^2 \\ X_{2stat} &= \tfrac{1}{2}\rho_w L T C_2(\psi_{cr})V_{cr}^2 \\ X_{6stat} &= \tfrac{1}{2}\rho_w L^2 T C_6(\psi_{cr})V_{cr}^2 \end{aligned} \tag{21}$$

being the steady relative current forces/moment, while $\psi_{cr} = \arctan(-v_r/-u_r)$ is the relative current direction. The dynamic contribution is assumed to be:

$$\begin{aligned} X_{1dyn} &= - (a_{22}-a_{11})V_c \sin(\psi_c-x_6)\dot{x}_6 + X_{1D} \\ X_{2dyn} &= - (a_{22}-a_{11})V_c \cos(\psi_c-x_6)\dot{x}_6 + X_{2D} \\ X_{6dyn} &= + X_{6D} \end{aligned} \tag{22}$$

which consists of a potential and a viscous part.

Both the viscous steady current forces/moment and the viscous part of the dynamic contributions can be determined by model tests.

6.1 Viscous damping in current due to the sway and yaw mode of motion

In order to determine the dynamic contributions X_{1dyn}, X_{2dyn} and X_{6dyn} caused by the sway and yaw modes of motion, Planar Motion

Mechanism tests for various current speeds, angles of current attack and frequencies were carried out. The test set-up and the test procedure have been reported in ref. [7]. Besides the dynamic contributions also the steady current forces have been determined.

6.1.1 Current force coefficients

Since a part of the low frequency viscous damping are related to the steady current forces/moment, first the measured steady current forces/moment will be presented. In Fig. 10 the sign convention of the current forces and moment, ship's heading and current direction is given.

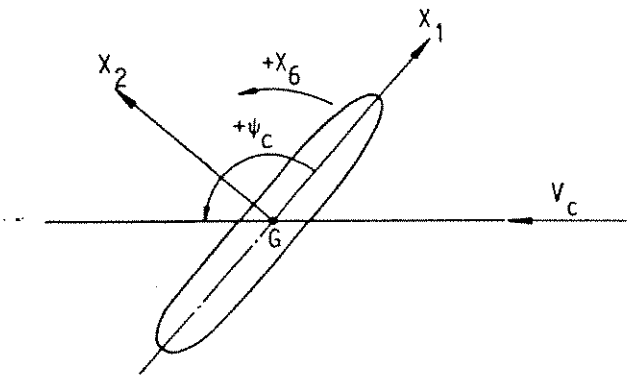

Fig. 10. Sign convention for current forces

The current data presented as the non-dimensional resistance coefficients for the 200 kTDW tanker are shown in Fig. 11. The data concern the loaded and the ballasted condition for a water depth of 82.5 m.

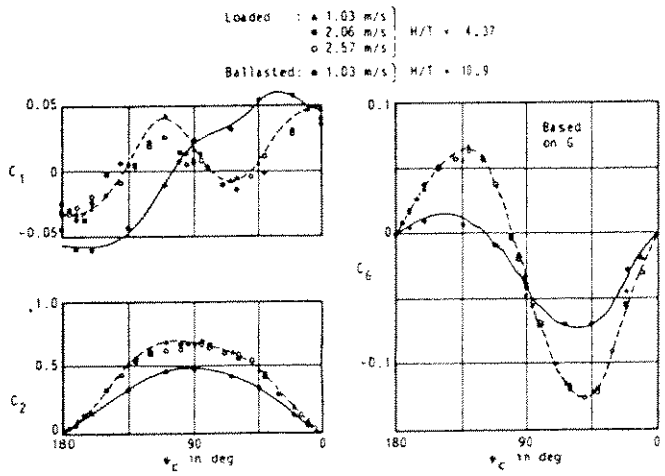

Fig. 11. The current force/moment coefficients

The non-dimensional coefficients have been obtained as follows:

$$C_1(\psi_c) = \frac{X_1(\psi_c)}{\frac{1}{2}\rho_w L T V_c^2} \quad \text{(longitudinal direction)}$$

$$C_2(\psi_c) = \frac{X_2(\psi_c)}{\frac{1}{2}\rho_w L T V_c^2} \quad \text{(transverse direction)}$$

$$C_6(\psi_c) = \frac{X_6(\psi_c)}{\frac{1}{2}\rho_w L^2 T V_c^2} \quad \text{(yaw direction)} \qquad (23)$$

in which:
ψ_c = undisturbed current direction
V_c = undisturbed current velocity
L = length between perpendiculars of the tanker
T = draft of the tanker
ρ_w = specific density of sea water = $0.1045\ tfs^2m^{-4}$.

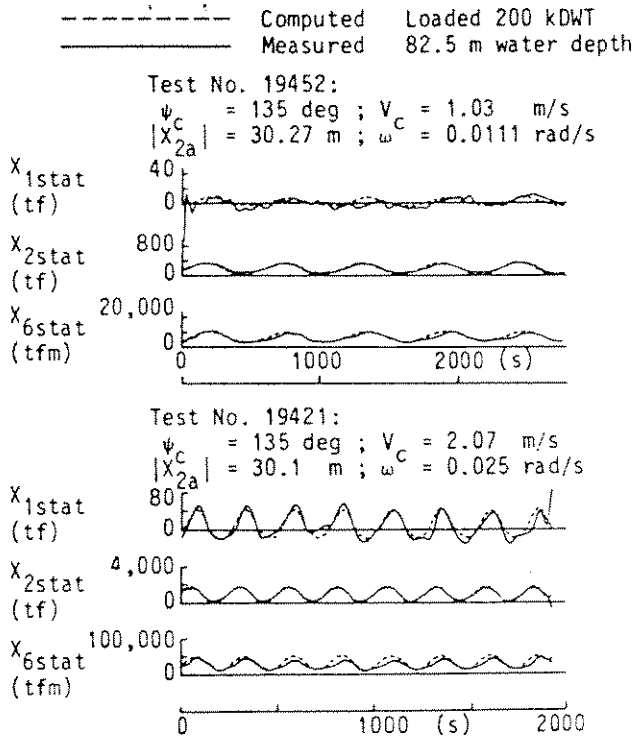

Fig. 12. Computed and measured steady relative current force and moment components

6.1.2 Relative current force concept for the surge and sway mode of motion

Based on the known oscillating sway displacement and frequency of the oscillaton, the known added mass coefficients and the

inertia properties of the vessel, the relative current force and moment components X_{1stat}, X_{2stat} and X_{6stat} respectively can be derived from the measurements following eq. (20). The dynamic contributions are assumed to be dependent on the yaw velocity. For some specific conditions the results of the derived measurements are presented in Fig. 12. In Fig. 12 also the results have been plotted of the computed steady relative current force and moment components following eq. (21). The coefficients used for the computations were obtained from Fig. 11.

From the results it can be concluded that the application of the steady relative current force concept will satisfy.

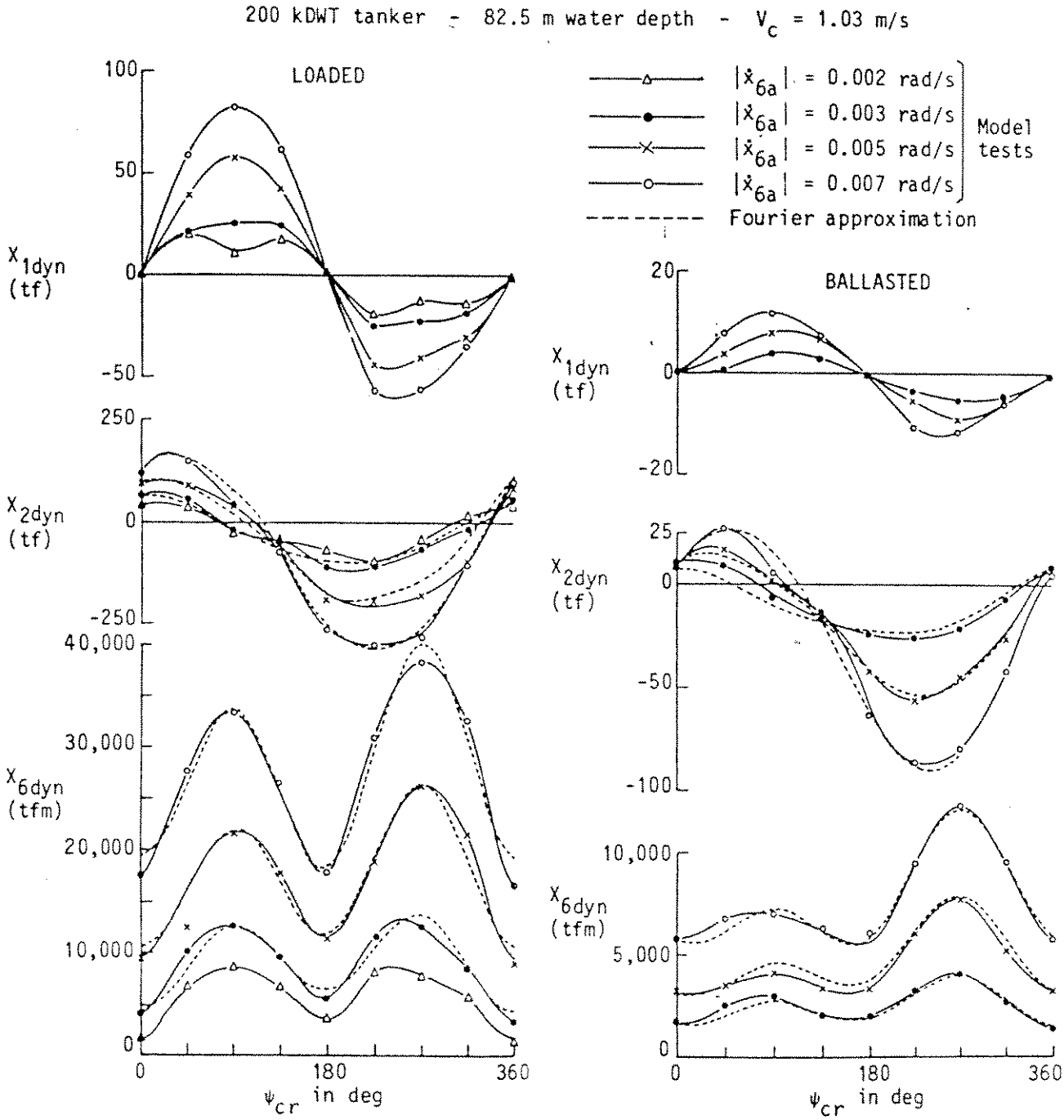

Fig. 13. Dynamic current contribution in surge, sway and yaw direction due to motion in yaw direction

6.1.3 Derivation of the dynamic current contributions

Based on the known oscillating motion, the measured oscillating forces/moment and the measured steady resistance forces/moment the dynamic current contributions were derived. For some conditions the derived dynamic current contributions in surge, sway and yaw direction respectively X_{1dyn}, X_{2dyn} and X_{6dyn} are given in Fig. 13.

The results of the dynamic current contribution were analyzed by means of Fourier theory. In terms of Fourier coefficients the dynamic contributions can be written as follows:

$$X_{1dyn} = \{C_{01} + \sum_{n=1}^{N} C_{n1} \cos(n\psi_{cr}) + S_{n1} \sin(n\psi_{cr})\} \tfrac{1}{2}\rho_w L T V_{cr}^2$$

$$X_{2dyn} = \{C_{02} + \sum_{n=1}^{N} C_{n1} \cos(n\psi_{cr}) + S_{n2} \sin(n\psi_{cr})\} \tfrac{1}{2}\rho_w L T V_{cr}^2$$

$$X_{6dyn} = \{C_{06} + \sum_{n=1}^{N} C_{n6} \cos(n\psi_{cr}) + S_{n6} \sin(n\psi_{cr})\} \tfrac{1}{2}\rho_w L^2 T V_{cr}^2 \qquad (24)$$

in which:

$\psi_{cr} = \arctan(-v_r/-u_r)$

$V_{cr} = (u_r^2+v_r^2)^{\frac{1}{2}}$

$C_{nj} = C_{nj}(\dot{x}_6 L/V_{cr})$

$= C_{nj}(r')$ $\quad (j = 1,2,6)$

$S_{nj} = C_{nj}(r')$ $\quad (j = 1,2,6)$

while further:

$C_{nj} = a_{nj} + b_{nj}r' + c_{nj}r'|r'|$

$S_{nj} = d_{nj} + e_{nj}|r'| + f_{nj}r'^2$

Some results of the analysis of the Fourier coefficients for the lateral force component are given in Fig. 14. From the analyzed results it was derived that the dynamic current contributions due to yaw motion can be described as follows:

$$X_{1dyn} = -0.4(a_{22}-a_{11}) \sin\psi_{cr} V_c \dot{x}_6$$

$$X_{2dyn} = -(a_{22}-a_{11}) \cos\psi_{cr} V_c \dot{x}_6 + X_{2D}$$

$$X_{6dyn} = X_{6D} \qquad (25)$$

in which:

$$X_{2D} = \{X'_{2Vr} V_{cr} \dot{x}_6 + X'_{2V|r|} V_{cr} |\dot{x}_6| + X'_{2r^2} L \dot{x}_6^2 + X'_{2r|r|} L \dot{x}_6 |\dot{x}_6| + X'_{2r^3/V} \dot{x}_6^3 L^2/V_{cr} + X'_{2|r^3|/V} |\dot{x}_6|^3 L^2/V_{cr}\} \tfrac{1}{2}\rho_w L^2 T$$

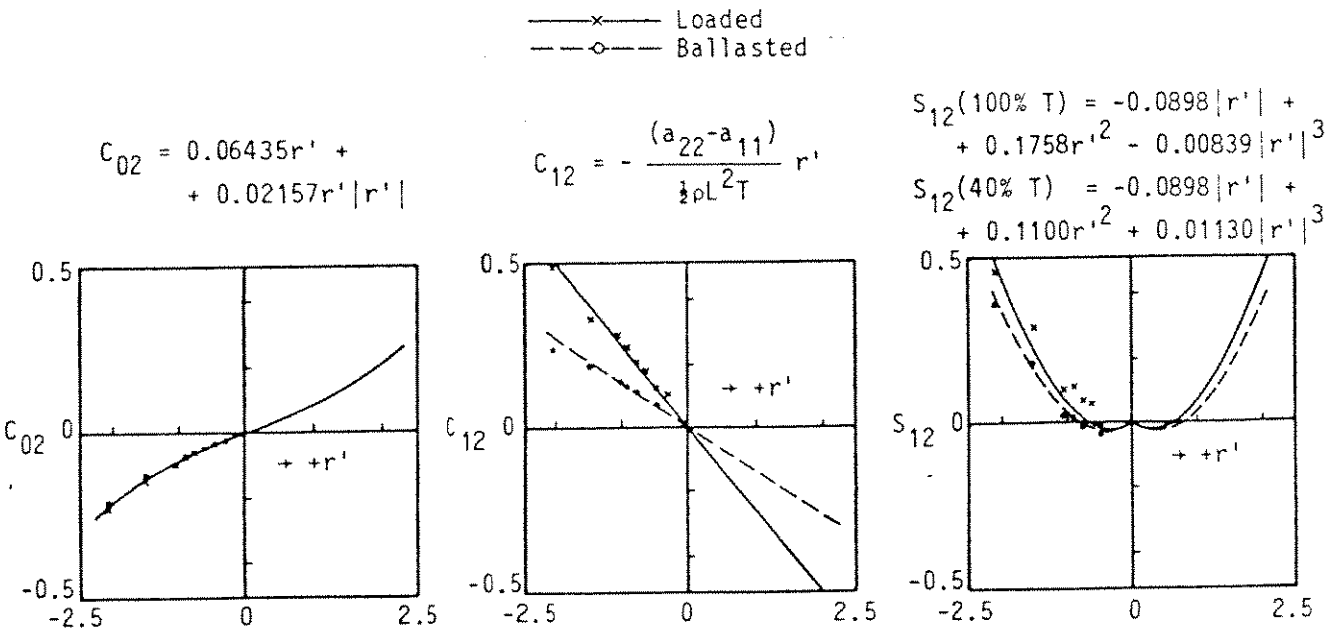

Fig. 14. Some examples of the derivation of the coefficients of the dynamic current contribution in sway direction due to motion in yaw direction

and

$$X_{6D} = \{X'_{6Vr}\, V_{cr}\, \dot{x}_6 + X'_{6V|r|}\, V_{cr}\, |\dot{x}_6| + X'_{6r^2}\, L\, \dot{x}_6 + X'_{6r|r|}\, L\, \dot{x}_6\, |\dot{x}_6| + X'_{6r^3/V}\, \dot{x}_6^3\, L^2/V_{cr} + X'_{6|r^3|/V}\, |\dot{x}_6|^3\, L^2/V_{cr}\}\tfrac{1}{2}\rho_w L^3 T$$

By means of the derivation of the dynamic current coefficients the viscous part can be described. In terms of Fourier coefficients for the lateral force we obtain the following coefficients:

$$X'_{2Vr} = 0.06435 - 0.03996 \cos 2\psi_{cr} + 0.02654 \cos 3\psi_{cr} + (0.00683 \cos 2\psi_{cr} + 0.06634 \cos 3\psi_{cr})Q$$

$$X'_{2V|r|} = (-0.0898 + 0.1309\, Q)\sin \psi_{cr}$$

$$X'_{2r^2} = (0.1100 - 0.1527\, Q)\sin \psi_{cr}$$

$$X'_{2r|r|} = 0.02157 + 0.01484 \cos 2\psi_{cr} - 0.03886 \cos 3\psi_{cr} + (-0.00838 \cos 2\psi_{cr} - 0.10804 \cos 3\psi_{cr})Q$$

$$X'_{2r^3/V} = (0.01168 + 0.03286\, Q)\cos 3\psi_{cr}$$

$$X'_{2|r^3|/V} = (0.0113 + 0.05801\, Q)\sin \psi_{cr}$$

In a similar way the coefficients for the moment were derived.

It is assumed that the coefficients are linearly proportional to the draft of the vessel. The factor Q used for the interpolation can be formulated as:

$$Q = (T-T40)/(T100-T40)$$

Some examples of comparison between Fourier approximations and test results are given in Fig. 13.

Knowing the description of the resistance force and moment components time domain simulations can be carried out in a current field.

7. BOW HAWSER MOORED TANKER EXPOSED TO CURRENT

To evaluate the derived resistance force and moment components in current low frequency motion decay simulations of a tanker (3 D.O.F.) moored by means of a bow hawser and exposed to current only were carried out. The simulations are compared with the results of model tests. The tanker concerns the fully and intermediate loaded 200 kTDW tanker moored in 82.5 m water depth. The bow hawser was connected to a fixed pile. For both the computations and the model tests unloaded lengths of 45 and 75 m were applied. The non-linear load deflection curve\ as used for both hawsers is presented in Fig. 6. The current speeds were 2 and 3 knots.

7.1 Computations

Considering eq. (6), (20), (21) and (22) the complete equations of motion can be written as follows:

$$\begin{aligned}
&(M+a_{11})\ddot{x}_1 = \\
&= (M+a_{22})\dot{x}_2\dot{x}_6 + X_{1stat} + X_{1dyn} + X_{1m} \\
&(M+a_{22})\ddot{x}_2 + a_{26}\ddot{x}_6 = \\
&= -(M+a_{11})\dot{x}_1\dot{x}_6 + X_{2stat} + X_{2dyn} + X_{2m} \\
&(I_6+a_{66})\ddot{x}_6 + a_{62}\ddot{x}_2 = \\
&= X_{6stat} + X_{6dyn} + X_{6m} \qquad (26)
\end{aligned}$$

in which:

X_{1m}, X_{2m}, X_{6m} = mooring force/moment components caused by the bow hawser.

The current direction ψ_c as defined in Fig. 2 was 180 degrees. The values of the coefficients used for the potential inertia parts of the reaction forces/moment are given in Table 1. The coefficients for the steady relative current force/moment components are shown in Fig. 11. For the viscous part of the dynamic current contribution the coefficients are used as derived in the previous section.

7.2 Model tests

During the model tests the yaw motion of the tanker was measured only. The SPM tests were carried out in the Shallow Water Laboratory of MARIN measuring 210 by 17 m at a water depth of 1 m. The model scale was 1:82.5. The current speed of 2 and 3 knots was simulated by towing the set-up through the basin.

7.3 Results of computations and model tests

For the initial conditions for both the computations and the model tests the same values were used. In Fig. 15 the results of the motion decay as obtained from the simulations and the model tests are presented.

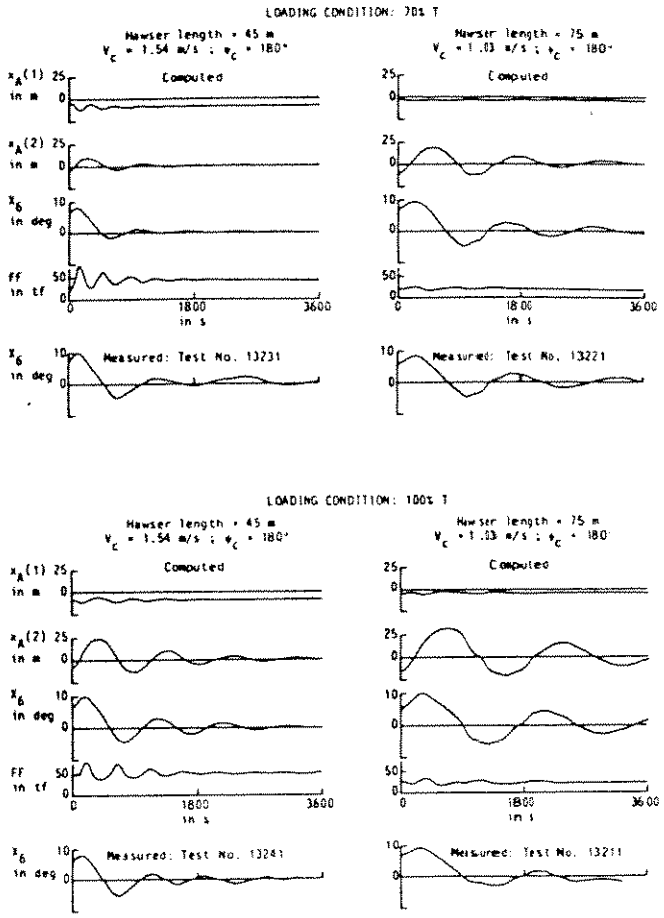

Fig. 15. Results of the motion decay tests in current

Sensitivity computations using the present formulation and the formulations given in ref. [5] and [6] showed that the value of the longitudinal steady relative current force, inspite of the very small value in relation to the other force/moment components will influence the decay of the motion in the horizontal plane. To fit the results of the model tests the longitudinal steady current force has been modified by a factor 2 and used for all computations.

In the mentioned cases the tanker performs stable decaying motions after the release from the initial start position. To evaluate the derived low frequency viscous terms in the equations of motion conditions have to be found that the tanker performs large amplitude unstable motions in the horizontal plane. By means of the Routh criterion the conditions for dynamic instability can be found.

8. LINEARIZED DYNAMIC STABILITY OF A HAWSER MOORED TANKER IN A CURRENT AND WIND FIELD

The procedure for the dynamic stability have been extensively presented and evaluated in ref. [12]. In the following the method will be briefly presented. For stable or unstable behaviour of the moored tanker a steady current and wind field will be considered. For the definitions reference is made to Fig. 2. The definitions of the dynamic stability in general is graphically shown in Fig. 16.

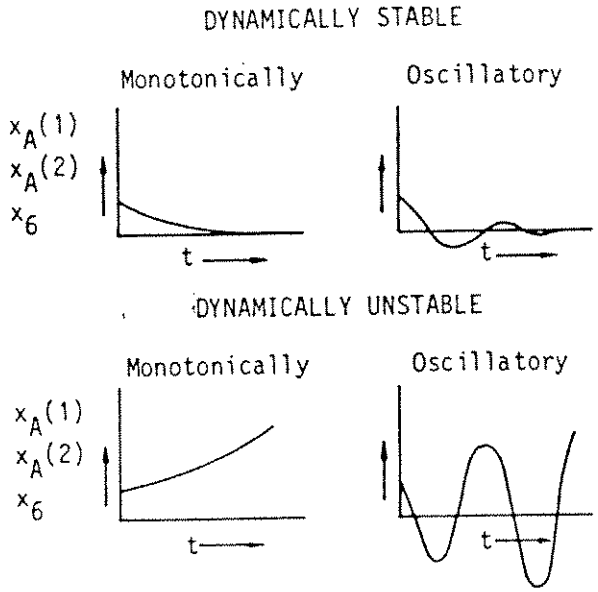

Fig. 16. Graphical representation of dynamic stability

For the determination of the stability or the instability of the system the characteristic equations have to be solved. The solution of the characteristic equations gives the motion characteristics due to small deviations about the static equilibrium position of the tanker in the considered steady current and wind field. To establish the equations of motion eq. (6) has to linearized. Linear equations of motion were obtained by means of a Taylor expansion to the first order yielding the following equations:

$$\sum_{j=1}^{6} (M_{kj}+a_{kj})\ddot{x}_j + b_{kjp}\dot{x}_j = X_{ke} + X_{km} + P_k$$

for $j = 1,2,6$ and $k = 1,2,6$ (27)

n which:

a_{kj} = added mass coefficients at low frequencies in k direction due to j mode of motion

b_{kjp} = potential damping coefficients at low frequencies

P_k = thruster force in k direction

nd

$$X_{ke} = X_{ke}(x_6(0)) + \frac{\partial X_{ke}(x_6(0))}{\partial x_j} x_j + \frac{\partial X_{ke}(x_6(0))}{\partial \dot{x}_j} \dot{x}_j$$

$$X_{km} = X_{km}(x_6(0)) + \frac{\partial X_{km}(x_6(0))}{\partial x_j} x_j + \frac{\partial X_{km}(x_6(0))}{\partial \dot{x}_j} \dot{x}_j$$

n which:

$X_k(x_6(0))$ = mean external force component in k direction due to wind and current

$X_{km}(x_6(0))$ = mean bow hawser force component in k direction

$x_6(0)$ = tanker heading in the equilibrium position

x_6 = tanker yaw with regard to the equilibrium heading $x_6(0)$.

Considering the linearized equations of motion about the equilibrium position and taking into account the appropriate coefficients we obtain:

$$\sum_{j=1}^{6} m_{kj}\ddot{x}_j + b_{kj}\dot{x}_j + c_{kj}x_j = 0$$

for k = 1,2,6 and J = 1,2,6 (28)

in which:

$x_j = A_j . e^{\sigma t}$

A_j = constant, dependent on the initial disturbance

σ = complex coefficient

$m_{kj} = M_{kj} + a_{kj}$

$$b_{kj} = -\frac{\partial X_{ke}}{\partial \dot{x}_j} + b_{kjp}$$

$$c_{kj} = -\frac{\partial X_{km}}{\partial x_j} - \frac{\partial X_{ke}}{\partial x_j}$$

The complex coefficient defines the characteristics of the motion. When the real part of σ is minus, the motion converges. The motion diverges in the plus case. Therefore, the condition of the motion can be determined by the sign of the real part of σ. Eq. (28) can be written as follows:

$$\sum_{j=1}^{6} m_{kj}A_j\sigma^2 + b_{kj}A_j\sigma + c_{kj}A_j = 0$$

for k = 1,2,6 and j = 1,2,6 (29)

or in matrix form:

$$[m\,\sigma^2 + b\,\sigma + c]\{A\} = 0 \qquad (30)$$

Since it is assumed that $\{A\} \neq 0$, eq. (30) will yield the following determinant:

$$|m\,\sigma^2 + b\,\sigma + c| = 0 \qquad (31)$$

On expansion this determinant may be arranged as:

$$S_6\sigma^6 + S_5\sigma^5 + S_4\sigma^4 + S_3\sigma^3 + S_2\sigma^2 + S_1\sigma + S_0 = 0 \qquad (32)$$

in which the coefficients symbolically for j = 1,2,6 are expressed as determinants:

$$S_6 = \begin{vmatrix} m_{1j} \\ m_{2j} \\ m_{3j} \end{vmatrix}$$

$$S_5 = \begin{vmatrix} m_{1j} \\ m_{2j} \\ b_{3j} \end{vmatrix} + \begin{vmatrix} m_{1j} \\ b_{2j} \\ m_{3j} \end{vmatrix} + \begin{vmatrix} b_{1j} \\ m_{2j} \\ m_{3j} \end{vmatrix}$$

$$S_4 = \begin{vmatrix} m_{1j} \\ m_{2j} \\ c_{3j} \end{vmatrix} + \begin{vmatrix} m_{1j} \\ b_{2j} \\ b_{3j} \end{vmatrix} + \begin{vmatrix} m_{1j} \\ c_{2j} \\ m_{3j} \end{vmatrix} + \begin{vmatrix} b_{1j} \\ m_{2j} \\ b_{3j} \end{vmatrix} + \begin{vmatrix} b_{1j} \\ b_{2j} \\ m_{3j} \end{vmatrix} + \begin{vmatrix} c_{1j} \\ m_{2j} \\ m_{3j} \end{vmatrix}$$

$$S_3 = \begin{vmatrix} m_{1j} \\ b_{2j} \\ c_{3j} \end{vmatrix} + \begin{vmatrix} m_{1j} \\ c_{2j} \\ b_{3j} \end{vmatrix} + \begin{vmatrix} b_{1j} \\ m_{2j} \\ c_{3j} \end{vmatrix} + \begin{vmatrix} b_{1j} \\ b_{2j} \\ b_{3j} \end{vmatrix} + \begin{vmatrix} b_{1j} \\ c_{2j} \\ m_{3j} \end{vmatrix} + \begin{vmatrix} c_{1j} \\ m_{2j} \\ b_{3j} \end{vmatrix} + \begin{vmatrix} c_{1j} \\ b_{2j} \\ m_{3j} \end{vmatrix}$$

$$S_2 = \begin{vmatrix} m_{1j} \\ c_{2j} \\ c_{3j} \end{vmatrix} + \begin{vmatrix} b_{1j} \\ b_{2j} \\ c_{3j} \end{vmatrix} + \begin{vmatrix} b_{1j} \\ c_{2j} \\ b_{3j} \end{vmatrix} + \begin{vmatrix} c_{1j} \\ m_{2j} \\ c_{3j} \end{vmatrix} + \begin{vmatrix} c_{1j} \\ b_{2j} \\ b_{3j} \end{vmatrix} + \begin{vmatrix} c_{1j} \\ c_{2j} \\ m_{3j} \end{vmatrix}$$

$$S_1 = \begin{vmatrix} b_{1j} \\ c_{2j} \\ c_{3j} \end{vmatrix} + \begin{vmatrix} c_{1j} \\ b_{2j} \\ c_{3j} \end{vmatrix} + \begin{vmatrix} c_{1j} \\ c_{2j} \\ b_{3j} \end{vmatrix}$$

$$S_0 = \begin{vmatrix} c_{1j} \\ c_{2j} \\ c_{3j} \end{vmatrix} \qquad (33)$$

Following the definitions in Fig. 2, the derivations as is indicated in ref. [12] and taking into account the coupling terms, the coefficients b_{kj} and c_{kj} can be written as follows:

$$b_{11} = 2X_{1c}(\psi_{cr})\frac{\cos\psi_{cr}}{V_c} + \\ - \frac{\partial X_{1c}(\psi_{cr})}{\partial\psi_{cr}}\frac{\sin\psi_{cr}}{V_c} + b_{11p}$$

$$b_{12} = 2X_{1c}(\psi_{cr})\frac{\sin\psi_{cr}}{V_c} + \\ + \frac{\partial X_{1c}(\psi_{cr})}{\partial\psi_{cr}}\frac{\cos\psi_{cr}}{V_c} + b_{12p}$$

$$b_{16} = 0.4(a_{22}-a_{11})V_c \sin\psi_{cr} + b_{13p}$$

$$b_{21} = 2X_{2c}(\psi_{cr})\frac{\cos\psi_{cr}}{V_c} + \\ - \frac{\partial X_{2c}(\psi_{cr})}{\partial\psi_{cr}}\frac{\sin\psi_{cr}}{V_c} + b_{21\ p}$$

$$b_{22} = 2X_{2c}(\psi_{cr})\frac{\sin\psi_{cr}}{V_c} + \\ + \frac{\partial X_{2c}(\psi_{cr})}{\partial\psi_{cr}}\frac{\cos\psi_{cr}}{V_c} + b_{22p}$$

$$b_{26} = (a_{22}-a_{11})V_c \cos\psi_{cr} + b_{26p}$$

$$b_{61} = 2X_{6c}(\psi_{cr})\frac{\cos\psi_{cr}}{V_c} + \\ - \frac{\partial X_{6c}(\psi_{cr})}{\partial\psi_{cr}}\frac{\sin\psi_{cr}}{V_c} + b_{31p}$$

$$b_{62} = 2X_{6c}(\psi_{cr})\frac{\sin\psi_{cr}}{V_c} + \\ + \frac{\partial X_{6c}(\psi_{cr})}{\partial\psi_{cr}}\frac{\cos\psi_{cr}}{V_c} + b_{32p}$$

$$b_{66} = \frac{\left[(L/2-FB)^3 + (L/2+FB)^3\right]}{3L} b_{22} + b_{33p}$$

(34)

$$C_{11} = CE\cos^2\gamma + \frac{FF}{LE}\sin^2\gamma$$

$$C_{12} = \left(CE - \frac{FF}{LE}\right)\cos\gamma\sin\gamma$$

$$C_{16} = C_{12}\,AG + FF\sin\gamma - \frac{\partial X_{1e}(x_6(0))}{\partial x_6}$$

$$C_{21} = C_{21}$$

$$C_{22} = CE\sin^2\gamma + \frac{FF}{LE}\cos^2\gamma$$

$$C_{26} = C_{22}\,AG - FF\cos\gamma - \frac{\partial X_{2e}(x_6(0))}{\partial x_6}$$

$$C_{61} = C_{21}\,AG$$

$$C_{62} = C_{22}\,AG$$

$$C_{66} = (C_{22}\,AG - FF\cos\gamma)AG - \frac{\partial X_{6e}(x_6(0))}{\partial x_6}$$

(35)

in which:
$\gamma = \beta - x_6(0)$
LE = length of hawser with mean load in the equilibrium position
FF = mean hawser load in equilibrium position
CE = derivative of the static load deflection curve at position LE and FF
AG = longitudinal distance between centre of gravity and position of fairlead.

By varying parameters of the system and solving eq. (32) the convergence or divergence of the motion can be determined by the sign of the real part of σ. Of the six solutions, of which three are complex adjunctive, all real parts have to be negative for the motions to be convergent (stable).

8.1 Determination of the stability criterion

For the 200 kTDW tanker in loaded, intermediate and ballasted condition, respectively 100%, 70% and 40% of the loaded draft, the stability criterion has been determined. Therefore the tanker was exposed to a 2 knot current and 60 knot wind speed. The stability criterion was determined as function of hawser length and angle between current and wind. The static load-deflection curve of the hawser was assumed to be independent of the hawser length and is shown in Fig. 6.

For the computation of the coefficients use has been made of the mass coefficients as given in Table 1 (the potential damping coefficients are assumed to be zero), while for the derivatives of the current loads the results as presented in Fig. 11 were applied. For the wind loads on the tanker the data were used as presented by ref. [15]. The wind coefficients are presented in Fig. 17.

The results of the computed stability criterion is given in Fig. 18.

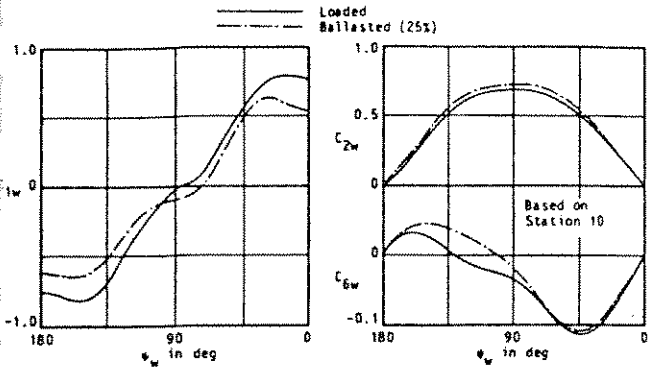

Fig. 17. The wind forces/moment coefficients (ref. [15])

. BOW HAWSER MOORED TANKER EXPOSED TO WIND AND CURRENT

In order to evaluate the equations of motion for the unstable behaviour of the bow ..er moored tanker in 2 kn current and 60 kn wind an unloaded hawser of 90 m has been chosen. From Fig. 18 it can be read that the 70% and 40% loaded condition exposed to the co-linearly directed specified wind and current will be in the unstable region.

Time domain simulations have been carried out and the results were compared with the results of the model test. Finally time domain simulations were carried to check the stability of the system for the 70% loading condition with an angle of 45 and 90 degrees between the wind and the current, see Fig. 18.

The tanker with the specified loading conditions was moored in 82.5 m deep water and connected by means of the hawser to a fixed pile. The load-deflection curve of the 90 m long hawser is presented in Fig. 6.

Computations

Following eq. (6) and eq. (20) the complete equations of motion can be written as follows:

$$(M+a_{11})\ddot{x}_1 =$$

$$= (M+a_{22})\dot{x}_2\dot{x}_6 + X_{1stat} + X_{1dyn} + X_{1w} + X_{1m}$$

$$(M+a_{22})\ddot{x}_2 + a_{26}\ddot{x}_6 =$$

$$= -(M+a_{11})\dot{x}_1\dot{x}_6 + X_{2stat} + X_{2dyn} + X_{2w} + X_{2m}$$

$$(I_6+a_{66})\ddot{x}_6 + a_{62}\ddot{x}_2 =$$

$$= X_{6stat} + X_{6dyn} + X_{6w} + X_{6m} \qquad (36)$$

in which:

X_{1w}, X_{2w}, X_{6w} = the steady wind forces/moment components.

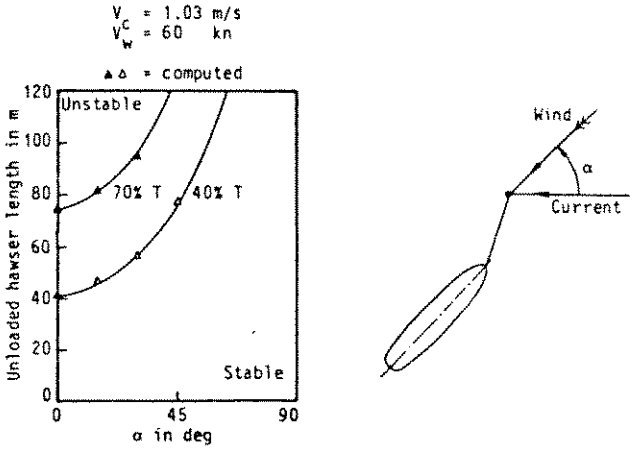

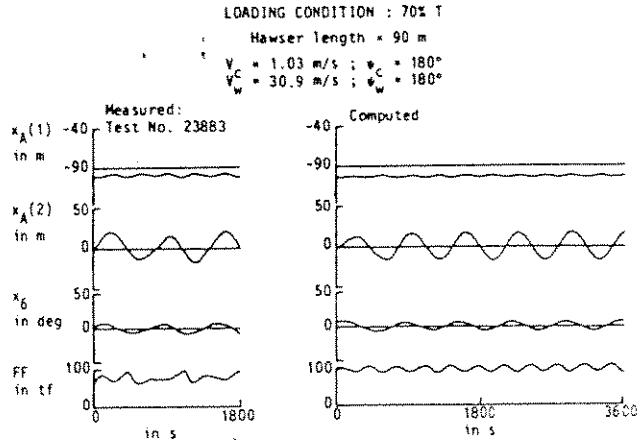

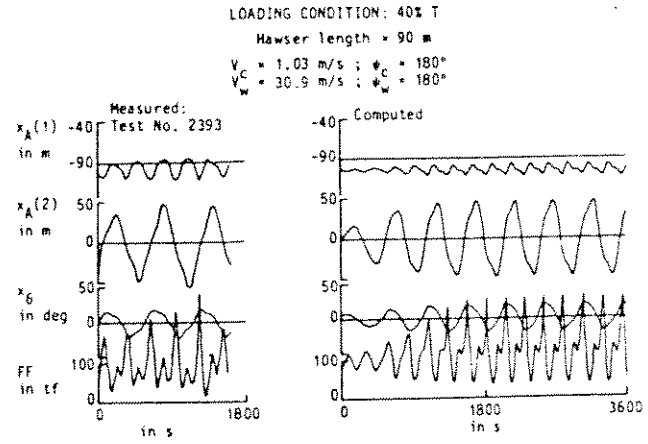

Fig. 18. Computed and measured behaviour of unstable SPM system

The wind forces are defined as follows see Table 1):

$$_{1w} = \tfrac{1}{2}\rho_A C_{1w}(\psi_{wr})\{A_{TS} + (H-T)B\}V_{wr}^2$$

$$_{2w} = \tfrac{1}{2}\rho_A C_{2w}(\psi_{wr})\{A_{LS} + (H-T)L\}V_{wr}^2$$

$$_{6w} = \tfrac{1}{2}\rho_A C_{6w}(\psi_{wr})\{A_{LS} + (H-T)L\}L\, V_{wr}^2 +$$

$$- X_{2w}\, FB \qquad (37)$$

n which:
A = specific density of air = .
= 0.00013 tfs^2m^{-4}.

For the definition of the system of coordinates and the weather directions, see ig. 2.

The values of the coefficients used for he potential inertia parts of the reaction orces/moment are given in Table 1, while he potential damping coefficient $b_{kjp}=0$. he coefficients for the steady relative urrent and wind force/moment components are hown in Fig. 11 and Fig. 15 respectively. or the viscous part of the dynamic current ontribution the coefficients are used as ndicated in section 6.1.3.
ll computations have been carried out by sing the ACSL-packet, see ref. [14] and xecuted on the Cyber 855 of MARIN.

.2 Model tests

During the model tests the horizontal otions at point A (= fairlead) were meaured in an earth-fixed system of co-ordiates as indicated in Fig. 2. Furthermore he yaw motion and the hawser force were ecorded. Both the linear and the rotational otions were measured by means of optical racking devices.

The SPM model tests were carried out in he Wave and Current Laboratory MARIN measuring 60 by 40 m at a water depth of 1 m. he model scale was 1:82.5.

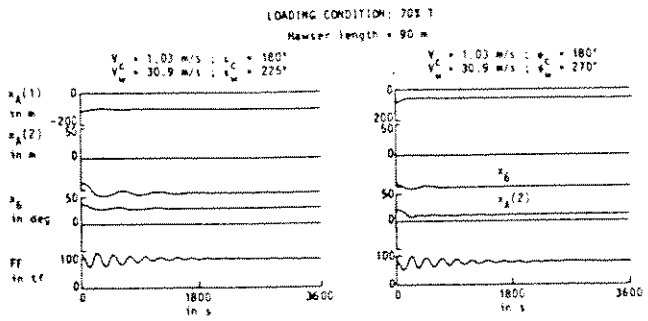

Fig. 19. Computed behaviour of a stable SPM system

9.3 Results of computations and model tests

In Fig. 18 the comparison of the results of the simulations and the model test for the unstable tanker conditions are presented.

As a result of the unstable behaviour of the ballasted tanker the dynamic loads in the hawser increase up to 250 tf instead of 87 tf as results from the static calculation. The computed result of the stable conditions with the 70% loaded tanker are shown in Fig. 19. In these conditions the model tests showed a stable behaviour of the system also. The measured and computed equilibrium positions are shown in Fig. 20. A good agreement was found between the computed and measured results.

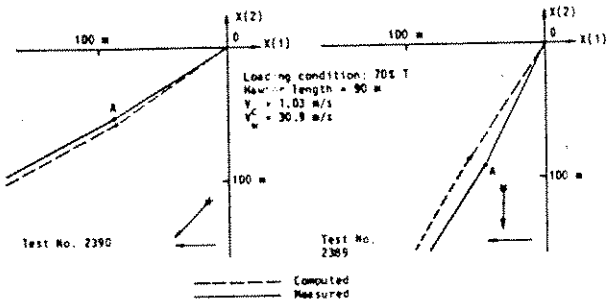

Fig. 20. Computed and measured stable equilibrium position of the stable SPM system

10. CONCLUSIONS

Because an SPM moored tanker will slowly oscillate in the coupled mode of natural frequencies, knowledge of the low frequency hydrodynamic viscous damping force/moment components in the equations of motion is of importance. Based on experimental data low frequency resistance coefficients have been derived. Evaluation of the derived formulation on the low frequency viscous damping in the equations of motion gives satisfactory results. From the results it can be concluded that distinction has to be made between the damping force/moment components for no-current and current condition.

By using the linearized form of the equations of motion the instability of an SPM system in current condition can be studied. Applying thereafter the non-linear equations of motion it can be concluded that the stability procedure indicates good results.

FERENCES

1. Wichers, J.E.W., "On the Low Frequency Surge Motions of Vessels Mooring in High Seas", OTC Paper 4437, 1982.
2. Huijsmans, R.H.M. and Hermans, A.J., "A Fast Algorithm for Computation of 3-D Ship Motions at Moderate Forward Speed", 4th International Conference on Numerical Ship Hydrodynamics, Washington, 1985.
3. Huijsmans, R.H.M. and Wichers, J.E.W., "Considerations on Wave Drift Damping of a Moored Tanker for Zero and Non-Zero Drift Angle", PRADS, Trondheim, June 1987.
4. Wichers, J.E.W., "Slowly Oscillating Mooring Forces in Single Point Mooring Systems", BOSS'79, London, August 1979.
5. Molin, B. and Bureau, G., "A Simulation Model for the Dynamic Behaviour of Tankers Moored to SPM", International Symposium on Ocean Engineering and Ship Handling, Gothenburg, 1980.
6. Obokata, J., "Mathematical Approximation of the Slow Oscillation of a Ship Moored to Single Point Moorings", Marintec Offshore China Conference, Shanghai, October 23-26, 1983.
7. Wichers, J.E.W., "Progress in Computer Simulations of SPM Moored Vessels", OTC Paper 5175, 1986.
8. Van Oortmerssen, G., "The Motions of a Moored Ship in Waves", MARIN publication, Wageningen, 1976.
9. Norrbin, N.H., "Theory and Observations of the Use of a Mathematical Model for a Ship's Manoeuvring in Deep and Confined Waters", Proceedings 8th Symposium on Naval Hydrodynamics, 1970.
10. Wichers, J.E.W. and Van Sluijs, M.F., "The Influence of Waves on the Low Frequency Hydrodynamic Coefficients of Moored Vessels", OTC Paper 3625, 1979.
11. Pinkster, J.A., "Low Frequency Second Order Wave Exciting Forces on Floating Structures", MARIN publication, Wageningen, 1980.
12. Wichers, J.E.W., "On the Slow Motions of Tankers Moored to Single Point Mooring Systems", OTC Paper 2548, 1976.
13. Remery, G.F.M. and Van Oortmerssen, G., "The Mean Wave, Wind and Current Forces on Offshore Structures and their Role in the Design of Mooring Systems", OTC Paper 1741, 1973.
14. Mitchell, E.E.L. and Gauthier, J.S., "Advanced Continuous Simulation Language (ASCL)", Simulation, March 1976.